



Phonon Lasing in an Electromechanical Resonator

I. Mahboob,* K. Nishiguchi, A. Fujiwara, and H. Yamaguchi

NTT Basic Research Laboratories, NTT Corporation, Atsugi-shi, Kanagawa 243-0198, Japan

(Received 19 November 2012; published 18 March 2013)

An electromechanical resonator harboring an atomlike spectrum of discrete mechanical vibrations, namely, phonon modes, has been developed. A purely mechanical three-mode system becomes available in the electromechanical atom in which the energy difference of the two higher modes is resonant with a long-lived lower mode. Our measurements reveal that even an incoherent input into the higher mode results in coherent emission in the lower mode that exhibits all the hallmarks of phonon lasing in a process that is reminiscent of Brillouin lasing.

DOI: [10.1103/PhysRevLett.110.127202](https://doi.org/10.1103/PhysRevLett.110.127202)

PACS numbers: 85.85.+j, 05.45.-a, 42.65.Es, 42.65.Lm

A phonon laser has been a tantalizing prospect since the inception of lasers [1–4]. Although an optical emission can be easily selected and amplified by a photon cavity in a laser, the lack of discrete phonon transitions makes their selection and amplification by an equivalent phonon cavity a formidable challenge [2,3]. A recent approach to phonon lasing has been developed using optomechanical systems [5] in which the atomic level structure at the heart of a laser is supplanted with discrete optical modes whose transition energies correspond to parametrically coupled high-quality-factor mechanical modes [6,7]. Phonon lasing becomes available in this architecture by pumping the optical modes with a laser in a process akin to Raman or Brillouin lasing [6,8,9]. However, the unavoidable need for optical control in this compound architecture has the potential to hinder further development of the phonon laser as it imposes constraints in the natural habitat of phonons, namely, the solid-state system, which has to be compromised with an optical cavity.

In a variation on optomechanical systems, the possibility of coupling orthogonal mechanical oscillation modes in the same electromechanical resonator has recently emerged as the subject of intense interest [10–18]. Specifically, the intermodal coupling is generated by the motion of a given mode creating tension, which modifies the oscillation dynamics of all the other modes. This phenomenon can be exploited to mimic the physics of optomechanics [5,19,20] but uniquely with just phonons [13,15]. Consequently, this result opens up a path to purely mechanical lasing, where the discrete mode structure giving rise to the phonon emission is now also based on phonons which in turn eliminates the need for pumping with a laser [6,7].

The key to this approach is a three-mode system, where the frequency difference of two higher modes is commensurate with that of a lower mode [6,9]. However, electromechanical resonators usually uphold higher-order flexural modes that do not satisfy this condition [21]. One technically demanding approach to bypassing this limitation would be to mechanically couple three mechanical resonators whose natural frequencies satisfy this requirement. Here we show that a more natural alternative to this

objective becomes available when nonflexural mechanical oscillation modes are also considered.

The electromechanical resonator used in this study and shown in Fig. 1(a) integrates piezoelectric transducers into the mechanical element and has previously been utilized to explore nonlinear phenomena [15,22,23]. The present device exhibits a fundamental flexural mode $\omega_L/2\pi = 174470$ Hz with a damping rate $\gamma_L/2\pi = 1.1$ Hz as shown in Fig. 1(c). Remarkably, a further 200 mechanical oscillation modes are also identified up to 4 MHz as shown in Fig. 1(b) by simply expanding the homodyne measurement bandwidth. The resonant response of these modes exhibits both amplitude and phase with respect to the drive, thus confirming them as harmonic oscillations [21]. Finite element analysis reveals that the mechanical oscillator sustains, in addition to the well-known flexural modes, torsional modes and modes composed of the etched overhangs [24]. The experimentally observed spectrum shown in Fig. 1(b) is thus mostly composed of admixtures of different order flexural-torsional-overhang oscillations [24].

The broadband response of the electromechanical resonator resembles an atom where the different oscillation modes play the role of electron levels. Strikingly, the electromechanical atom harbors numerous three-mode systems as described above [24]. The three-mode combination selected in this study consists of the lower mode ω_L shown in Fig. 1(c), the middle mode $\omega_M/2\pi = 2345077$ Hz with $\gamma_M/2\pi = 24.4$ Hz, and the higher mode $\omega_H/2\pi = 2519512$ Hz with $\gamma_H/2\pi = 34$ Hz shown in Figs. 1(d) and 1(e), respectively, which results in $\omega_H - \omega_M = \omega_L - \Delta$ where $\Delta/2\pi = 35$ Hz.

First in order to investigate the coupling between the three modes, the higher order mode is excited but this results in no output signal in the vicinity of the lower and middle modes as $\omega_L \neq \omega_H - \omega_M$ with $\Delta > \gamma_L, \gamma_M$ and γ_H . However, the piezoelectric transducer can also impart static strain to the mechanical element, enabling its resonance frequency to be tuned [22,25]. As a result $\omega_L/2\pi$ can be reduced by ~ 25 Hz with the application of negative bias as shown in Fig. 2(a), which results in

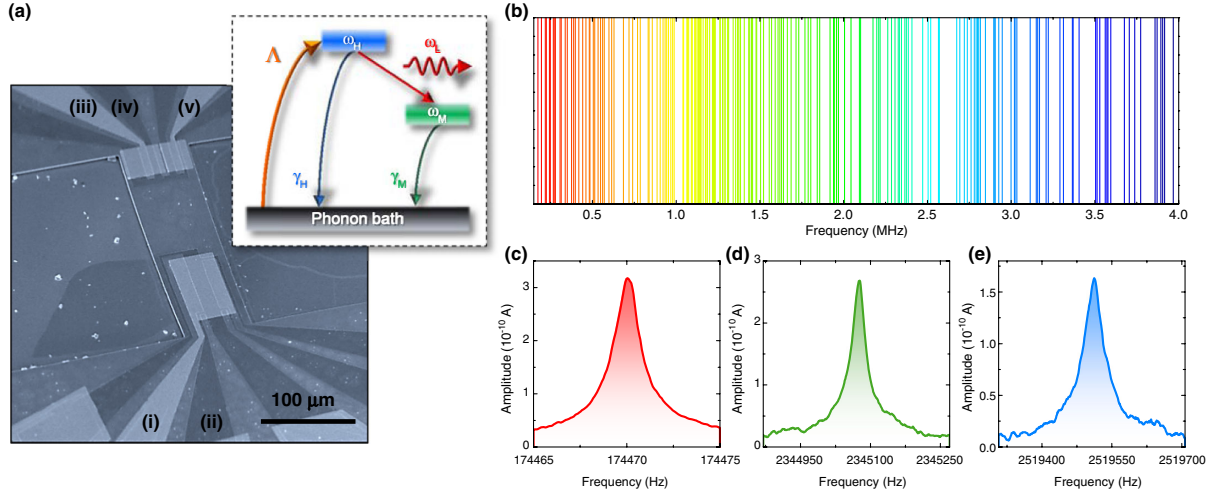


FIG. 1 (color online). (a) An electron micrograph of the electromechanical resonator which incorporates a two-dimensional electron gas (ii and iv) above which Schottky-contacted gold electrodes are placed (i, iii, and v). The mechanical vibrations are piezoelectrically excited by gate (i) which are then detected by the motion induced piezovoltage from gate (iii) at 2.0 K and 10^{-7} mbar, where contacts (ii), (iv), and (v) are grounded. The inset schematically depicts the phonon-lasing protocol. (b) Harmonically probing the electromechanical resonator reveals almost 200 resonances up to 4 MHz, where each line in this plot corresponds to a mechanical vibration. The three-mode system consists of the fundamental flexural oscillation as the lower mode ω_L (c) where the middle mode ω_M (d) and the higher mode ω_H (e) are composite oscillations [24]. The three modes are harmonically probed with amplitudes of $100 \mu\text{V}_{\text{rms}}$, $5 \text{ mV}_{\text{rms}}$, and $8 \text{ mV}_{\text{rms}}$, respectively.

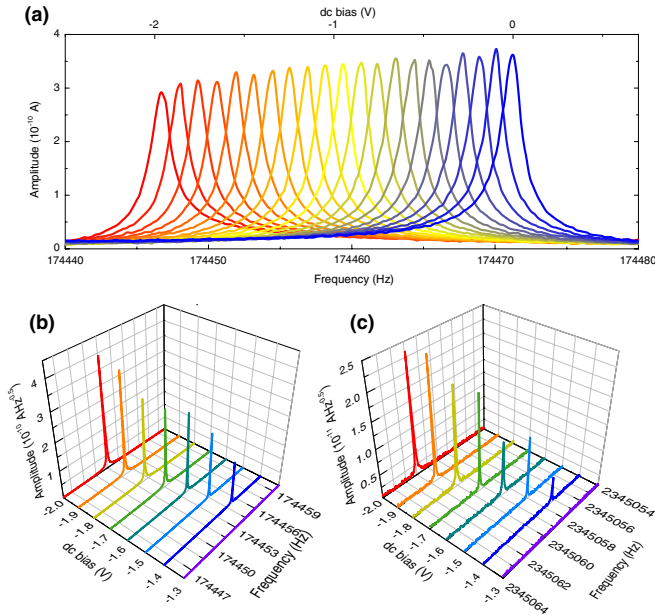


FIG. 2 (color online). (a) The application of dc bias to electrode (i) in addition to a $100 \mu\text{V}_{\text{rms}}$ harmonic probe can be used to tune the frequency of the lower mode. Although the flexural and torsional modes can be affected by the resultant piezoelectric strain, the composite modes (ω_M and ω_H) show no discernible response possibly due to their larger bandwidths. (b) and (c) The current noise spectral density around the lower and middle modes in response to a $60 \text{ mV}_{\text{rms}}$ harmonic tone applied at exactly ω_H reveals the creation of mechanical vibrations namely phonon emission as dc bias is applied to the electromechanical resonator to reduce ω_L .

$\Delta < \gamma_M$ and γ_H . Figures 2(b) and 2(c) show the output noise spectra collected around the lower and middle modes as a function of the bias voltage applied to the electromechanical resonator while a single harmonic tone is simultaneously activated at exactly ω_H . Notably, as a more negative bias voltage is applied, a larger output signal (i.e., spontaneous phonon emission or a mechanical vibration) is observed in both the lower and middle modes from just a single input into the higher mode. These observations vividly demonstrate the presence of intermodal coupling, which mediates energy transfer between the modes. For all subsequent measurements, the maximum available bias voltage of -2.0 V is used.

Next the dynamics of the phonon emission in the lower and middle modes are investigated as a function of the amplitude of the harmonic tone applied at ω_H . The results of this measurement shown in Figs. 3(a)–3(c) reveals the phonon emission in both the lower and middle modes has a clear threshold followed by region of linear rise which saturates at large tone amplitudes and is discussed later [6,7]. In addition, the phonon emission in the lower and middle modes undergoes dispersion to higher and lower frequencies, respectively, as shown in Figs. 3(a) and 3(b), but their sum frequency corresponds to the input tone at ω_H as shown in Fig. 3(e). The observed dispersion arises from the displacement of the higher mode which modifies the tension in the electromechanical resonator.

Ostensibly, this process resembles Raman or Brillouin lasing, which is typically composed of one phonon and two photons, as both energy and momentum are difficult to conserve with only photons rendering all-photon

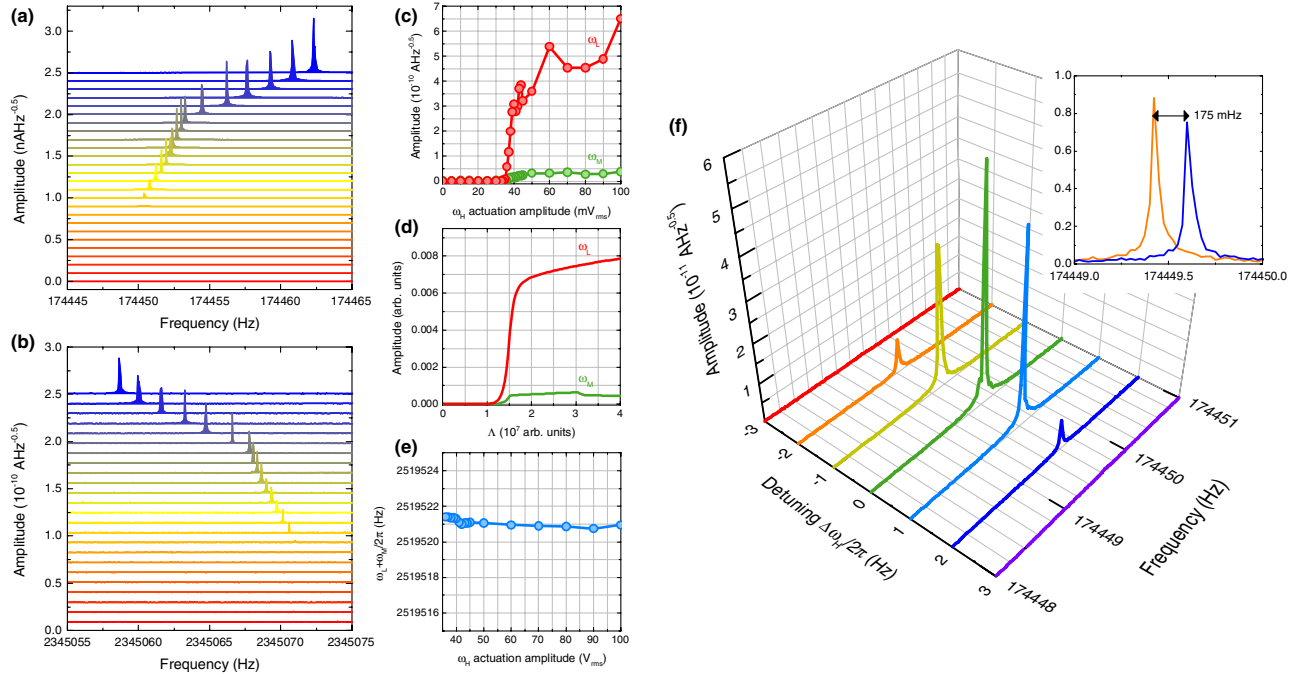


FIG. 3 (color online). (a) and (b) The current noise spectral density around the lower and middle modes, respectively in response to a 0–100 mV_{rms} harmonic tone applied at exactly ω_H . The spectra are offset for clarity with the bottom (top) spectrum corresponding to 0 mV_{rms} (100 mV_{rms}) where the amplitude of the tone is nonuniformly varied. (c) The corresponding amplitudes of the phonon emission in the lower and middle modes. (d) The calculated amplitudes of the phonon emission in the lower and middle modes in response to the harmonic tone. (e) The sum frequency of the phonon emission in the lower and middle modes. (f) The phonon emission in the lower mode is confined within 175 mHz (the inset shows the phonon emission when the detuning is $\omega_H \pm 2$ Hz), which is much less than $\gamma_L/2\pi$ when the harmonic tone with an amplitude of 36 mV_{rms} is detuned around ω_H with a measurement resolution bandwidth of 25 mHz.

three-wave mixing improbable [6,8,9]. However, in contrast, energy conservation is satisfied in the electromechanical three-mode system with $\hbar\omega_H = \hbar\omega_M + \hbar\omega_L$ as the spatial confinement of the three modes breaks their translational symmetry which relaxes the need for momentum conservation and it uniquely makes three-wave mixing with phonons possible. More fundamentally, this process can be generalized as parametric resonance, where a pump phonon is annihilated to generate two phonons, the signal and the idler, which are degenerate [22,26,27]. In the present case, the nondegenerate analogue is realized where a ω_H phonon is annihilated to generate signal and idler phonons at different frequencies, namely, ω_L and ω_M . In reality, the tension created by exciting the higher mode [10–18], which in effect is modulating the spring constant of the electromechanical resonator, has components that can parametrically activate the lower and middle modes [22].

Accordingly, the total Hamiltonian of the system can thus be expressed as

$$H = \sum_n (P_n^2/2m_n + m_n\omega_n^2 X_n^2/2) - \Lambda X_H \cos(\omega_H t) - \kappa X_L X_M X_H, \quad (1)$$

where the terms in the summation correspond to the kinetic and potential energies of the modes with mass m_n that are defined by their canonical position X_n , momentum P_n , and $n = L, M$, and H for the lower, middle, and higher modes, respectively [6,8,27–29]. The second term describes the harmonic excitation of the higher mode with amplitude Λ . Lastly, although the intermodal coupling arises in the potential energy term, for generality the coupling has been expressed in the last term defined by the coupling constant κ .

This Hamiltonian yields the following equations of motion for the three-mode system:

$$\begin{aligned} X_L'' + \gamma_L X_L' + \omega_L^2 X_L (1 + \beta_L X_L^2) &= \kappa_L X_M X_H \\ X_M'' + \gamma_M X_M' + \omega_M^2 X_M (1 + \beta_M X_M^2) &= \kappa_M X_L X_H \\ X_H'' + \gamma_H X_H' + \omega_H^2 X_H (1 + \beta_H X_H^2) &= \Lambda \cos(\omega_H t) + \kappa_H X_L X_M \end{aligned} \quad (2)$$

which have been normalized by their respective modal masses, where dissipation terms and Duffing nonlinearities parametrized by γ_n and β_n have also been included [15,22]. Numerically solving Eq. (2) [24] indicates that the Duffing parameters determine the profile of the output oscillation amplitudes shown in Fig. 3(c), which yields $\beta_L = 10$, $\beta_M = 1$, and $\beta_H = 0.1$. On the other hand, the terms Λ and $\kappa_n = \kappa/m_n$ are bound by the ratio of the output oscillation amplitudes in the lower and middle modes, and the experimental result can be reproduced with $\kappa_n = 5 \times 10^8$ as shown in Fig. 3(d). This analysis reveals that the threshold to emission arises from not only the dissipation rate of the lowest mode (i.e., γ_L) but also from the displacement of the higher mode (i.e., X_H), which only turns on the intermodal coupling when it is driven sufficiently strongly by Λ . The calculation also indicates that the change in curvature observed in the phonon emission in the lower and middle modes originates from the Duffing nonlinearity of the lower mode (i.e., β_L), whereas the saturation in the phonon emission at large Λ arises from X_H quenching as the higher mode is ever more strongly coupled to the lower and middle modes.

Although a threshold to the phonon emission is a feature of lasing, a laser is fundamentally defined by its spectral purity [30]. To that end, the linewidth of the phonon emission in the lower mode is measured by detuning the harmonic tone applied to the higher mode. The result of this measurement shown in Fig. 3(f) definitively reveals

the phonon emission as being confined to a spectral range of 175 mHz. This is nearly 2 orders of magnitude less than the detuning range and almost an order of magnitude less than $\gamma_L/2\pi$, thus lending support to the emission being laserlike.

In order to investigate the details of the phonon-lasing line shapes further, white-noise voltage centered at ω_H with a bandwidth of $2\gamma_H$ is injected into the electromechanical resonator. The result of this excitation in the spectral region around the lower mode, shown in Fig. 4(a), reveals both that the output emission around ω_L has a threshold and that it is spectrally pure with a Gaussian line shape that has a width of only 80 mHz, just above the emission threshold. The emission linewidth as a function of the noise amplitude, shown in Fig. 4(b), also exhibits gain narrowing a characteristic feature of lasing [6,7,30]. Consequently a broadband incoherent input into the higher mode results in a spectrally pure, thus coherent, output in the lower mode. In contrast, the noise spectrum concurrently acquired in the vicinity of the middle mode yields no evidence for phonon lasing [24].

These measurements combined with the numerical solutions to Eq. (2) indicate that the condition $\gamma_H > \gamma_M \gg \gamma_L$ is a necessary prerequisite as it permits the higher mode to be excited sufficiently strongly so that it can activate the intermodal coupling while, simultaneously, the fast decay of the middle mode ensures that the lower mode is populated around ω_L . The resultant emission around ω_L is then

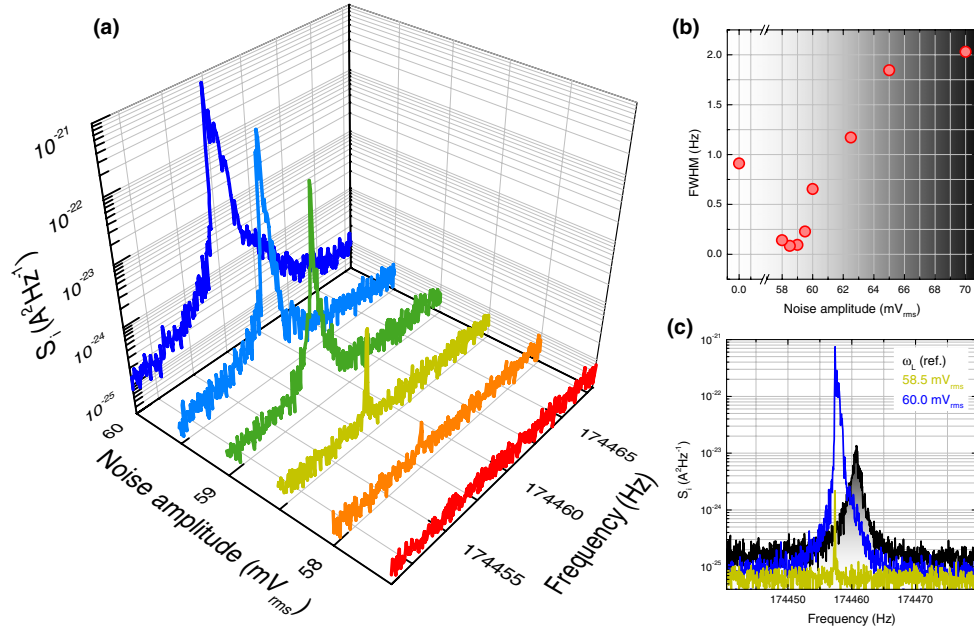


FIG. 4 (color online). (a) The noise power density around the lower mode in response to a white-noise voltage injected into the higher mode with a measurement resolution bandwidth of 25 mHz. (b) The corresponding full widths at half maximum (FWHM) extracted from Gaussian fits for noise amplitudes $< 60 \text{ mV}_{\text{rms}}$. For amplitudes $\geq 60 \text{ mV}_{\text{rms}}$, a composite function composed of a Gaussian and Lorentzian was used. (c) The experimental data and theoretical analysis [24] indicate the line shapes at larger noise amplitudes (60 mV_{rms}) originate from both the lasing (58.5 mV_{rms}) and the bandwidth of the lower mode (ref.). The ref. line shape of the lowest mode is measured by injecting white-noise voltage over $\omega_L \pm 25\gamma_L$ with an amplitude of only 100 μV_{rms} which also yields the 0 mV_{rms} data point in Fig. 4(b).

resonantly enhanced by the cavitylike lower mode, which yields the spectrally pure emission, i.e., lasing.

For larger noise amplitudes, the phonon emission linewidth broadens, and it can no longer be described by a Gaussian function as shown in Figs. 4(b) and 4(c). Analysis via Eq. (2) in these conditions reveals the bandwidth of the lower mode can also be activated in addition to the phonon lasing [24]. This results in a composite line shape composed of the Lorentzian from the lower mode and the Gaussian from the lasing as shown in Fig. 4(c). Specifically, the strong excitation of the higher mode results in a large phonon population at a range of frequencies close to ω_H . Whereas previously only the highest phonon density state at ω_H could contribute to the intermodal coupling and thus phonon lasing, the additional phonons around ω_H can now also activate the bandwidth of the lower mode, which can mask the lasing as shown in Figs. 4(a)–4(c). This phenomenon is analogous to power broadening observed in lasers [30].

These results herald the realization of a phonon laser in a purely mechanical architecture in a process analogous to Brillouin lasing. They also suggest exciting possibilities for the future [2–4,6,7], including cooling of the lowest mode by pumping the middle mode [6,28,31]. Furthermore, in contrast to degenerate parametric resonance in electromechanical resonators [22,26], the nondegenerate case developed here enables the signal and idler phonons to be distinguished via their energy. This suggests a path to investigating interference and correlation effects with phonons in analogy to photons generated by spontaneous parametric down-conversion, which have been used to demonstrate violation of Bell's inequality and are integral to quantum cryptography [29,32]. The potential to translate these ideas to phonons in electromechanical resonators provides a natural avenue for future research in light of mechanical resonators in their quantum ground state having been realized [19,20,33].

The authors are grateful to S. Miyashita for growing the heterostructure, D. Hatanaka for support, and N. Lambert, P.D. Nation, and F. Nori for discussions and comments. This work was partly supported by JSPS KAKENHI Grants No. 22226004 and No. 23241046.

*imran.mahboob@lab.ntt.co.jp

- [1] T. Maiman, *Nature (London)* **187**, 493 (1960).
- [2] J. Chen and J. B. Khurgin, *IEEE J. Quantum Electron.* **39**, 600 (2003).
- [3] J. B. Khurgin, *Physics* **3**, 16 (2010).
- [4] K. Vahala, M. Herrmann, S. Knünz, V. Batteiger, G. Saathoff, T. W. Hänsch, and T. Udem, *Nat. Phys.* **5**, 682 (2009).
- [5] T. J. Kippenberg and K. J. Vahala, *Science* **321**, 1172 (2008).
- [6] I. S. Grudin, H. Lee, O. Painter, and K. J. Vahala, *Phys. Rev. Lett.* **104**, 083901 (2010).
- [7] J. B. Khurgin, M. W. Pruessner, T. H. Stievater, and W. S. Rabinovich, *Phys. Rev. Lett.* **108**, 223904 (2012).
- [8] P. R. Hemmer and M. G. Prentiss, *J. Opt. Soc. Am. B* **5**, 1613 (1988).
- [9] G. Bahl, J. Zehnpfennig, M. Tomes, and T. Carmon, *Nat. Commun.* **2**, 403 (2011).
- [10] M. C. Cross, A. Zumdick, R. Lifshitz, and J. L. Rogers, *Phys. Rev. Lett.* **93**, 224101 (2004).
- [11] H. J. R. Westra, M. Poot, H. S. J. van der Zant, and W. J. Venstra, *Phys. Rev. Lett.* **105**, 117205 (2010).
- [12] I. Mahboob, Q. Wilmart, K. Nishiguchi, A. Fujiwara, and H. Yamaguchi, *Phys. Rev. B* **84**, 113411 (2011).
- [13] W. Venstra, H. Westra, and H. van der Zant, *Appl. Phys. Lett.* **99**, 151904 (2011).
- [14] A. Gaidarzhy, J. Dorignac, G. Zolfagharkhani, M. Imboden, and P. Mohanty, *Appl. Phys. Lett.* **98**, 264106 (2011).
- [15] I. Mahboob, K. Nishiguchi, H. Okamoto, and H. Yamaguchi, *Nat. Phys.* **8**, 387 (2012).
- [16] T. Faust, J. Rieger, M. J. Seitner, P. Krenn, J. P. Kotthaus, and E. M. Weig, *Phys. Rev. Lett.* **109**, 037205 (2012).
- [17] A. Eichler, M. del Álamo Ruiz, J. A. Plaza, and A. Bachtold, *Phys. Rev. Lett.* **109**, 025503 (2012).
- [18] K. J. Lulla, R. B. Cousins, A. Venkatesan, M. J. Patton, A. D. Armour, C. J. Mellor, and J. R. Owers-Bradley, *New J. Phys.* **14**, 113040 (2012).
- [19] J. D. Teufel, T. Donner, D. Li, J. W. Harlow, M. S. Allman, K. Cicak, A. J. Sirois, J. D. Whittaker, K. W. Lehnert, and R. W. Simmonds, *Nature (London)* **475**, 359 (2011).
- [20] J. Chan, T. P. M. Alegre, A. H. Safavi-Naeini, J. T. Hill, A. Krause, S. Groblacher, M. Aspelmeyer, and O. Painter, *Nature (London)* **478**, 89 (2011).
- [21] A. N. Cleland, *Foundations of Nanomechanics* (Springer-Verlag, Berlin, 2003).
- [22] I. Mahboob and H. Yamaguchi, *Nat. Nanotechnol.* **3**, 275 (2008).
- [23] I. Mahboob, E. Flurin, K. Nishiguchi, A. Fujiwara, and H. Yamaguchi, *Nat. Commun.* **2**, 198 (2011).
- [24] See Supplemental Material at <http://link.aps.org/supplemental/10.1103/PhysRevLett.110.127202> for details of the mode shapes, additional data and analysis.
- [25] S. C. Masmanidis, R. B. Karabalin, I. Vliaminck, G. Borghs, M. R. Freeman, and M. L. Roukes, *Science* **317**, 780 (2007).
- [26] K. L. Turner, S. A. Miller, P. G. Hartwell, N. C. MacDonald, S. H. Strogatz, and S. G. Adams, *Nature (London)* **396**, 149 (1998).
- [27] Y. R. Shen and N. Bloembergen, *Phys. Rev.* **137**, A1787 (1965).
- [28] M. Tomes, F. Marquardt, G. Bahl, and T. Carmon, *Phys. Rev. A* **84**, 063806 (2011).
- [29] K. J. McNeil and C. W. Gardiner, *Phys. Rev. A* **28**, 1560 (1983).
- [30] A. E. Siegman, *Lasers* (University Science Books, Sausalito, California, 1986).
- [31] G. Bahl, M. Tomes, F. Marquardt, and T. Carmon, *Nat. Phys.* **8**, 203 (2012).
- [32] R. Ghosh and L. Mandel, *Phys. Rev. Lett.* **59**, 1903 (1987).
- [33] A. D. O'Connell, M. Hofheinz, M. Ansmann, R. C. Bialczak, M. Lenander, E. Lucero, M. Neeley, D. Sank, H. Wang, M. Weides *et al.*, *Nature (London)* **464**, 697 (2010).